Metabolic Effects on Recombinant Interferon-γ Glycosylation in Continuous Culture of Chinese Hamster Ovary Cells

Gregg B. Nyberg,* R. Robert Balcarcel, Brian D. Follstad, Gregory Stephanopoulos, Daniel I. C. Wang

Department of Chemical Engineering, Biotechnology Process Engineering Center, Massachusetts Institute of Technology, Cambridge, Massachusetts 02139; telephone: (617) 253-4583; fax: (617) 253-3122; e-mail: gregstep@mit.edu

Received 22 January 1998; accepted 31 July 1998

Abstract: Asparagine linked (N-linked) glycosylation is an important modification of recombinant proteins, because the attached oligosaccharide chains can significantly alter protein properties. Potential glycosylation sites are not always occupied with oligosaccharide, and site occupancy can change with the culture environment. To investigate the relationship between metabolism and glycosylation site occupancy, we studied the glycosylation of recombinant human interferon-γ (IFN-γ) produced in continuous culture of Chinese hamster ovary cells. Intracellular nucleotide sugar levels and IFN-γ glycosylation were measured at different steady states which were characterized by central carbon metabolic fluxes estimated by material balances and extracellular metabolite rate measurements. Although site occupancy varied over a rather narrow range, we found that differences correlated with the intracellular pool of UDP-*N*-acetylglucosamine + UDP-*N*-acetylgalactosamine (UDP-GNAc). Measured nucleotide levels and estimates of central carbon metabolic fluxes point to UTP depletion as the cause of decreased UDP-GNAc during glucose limitation. Glucose limited cells preferentially utilized available carbon for energy production, causing reduced nucleotide biosynthesis. Lower nucleoside triphosphate pools in turn led to lower nucleotide sugar pools and reduced glycosylation site occupancy. Subsequent experiments in batch and fed-batch culture have confirmed that UDP-sugar concentrations are correlated with UTP levels in the absence of glutamine limitation. Glutamine limitation appears to influence glycosylation by reducing amino sugar formation and hence UDP-GNAc concentration. The influence of nucleotide sugars on site occupancy may only be important during periods of extreme starvation, since relatively large changes in nucleotide sugar pools led to only minor changes in glycosylation. *Biotechnol Bioeng* **62:** 336–347, 1999.
Keywords: metabolism; flux analysis; glycosylation; continuous culture; nucleotide sugars; interferon-γ

* *Present address:* Genetics Institute, One Burtt Road, Andover, MA 01810

Correspondence to: G. Stephanopoulos

Contract grant sponsors: National Science Foundation; National Institutes of Health

Contract grant numbers: EEC-94O2065; 5T 32GM08334

INTRODUCTION

Recombinant glycoproteins are typically produced in animal cells due to their post-translational processing capabilities. Animal cells characteristically glycosylate many secreted proteins, and this modification can significantly impact protein properties (Cumming, 1991; Goochee et al., 1992; Jenkins and Curling, 1994). The oligosaccharides of glycoproteins can influence protein folding (Helenius, 1994), trafficking (Fielder and Simons, 1995), biological activity (Berg et al., 1993), proteolytic stability (Sareneva et al., 1995), and clearance rate in vivo (Flesher et al., 1995). Thus the quality of recombinant protein depends upon the extent of glycosylation.

In this paper we focus in particular on N-linked glycosylation, i.e., the attachment of oligosaccharides to asparagine residues that are part of Asn-Xxx-Ser/Thr amino acid consensus sequences (Xxx is any amino acid except proline). The reaction sequence of N-linked glycosylation is known in detail (see reviews in Hirschberg and Snider (1987) and Kornfeld and Kornfeld (1985)). The initial steps involve the formation of an oligosaccharide precursor linked to dolichol, a membrane lipid. The precursor oligosaccharide is made up of sugars derived from activated sugar monomers (either nucleotide sugars or dolichol sugars that were formed from nucleotide sugars). The precursor oligosaccharide is subsequently transferred to a nascent polypeptide, typically as the polypeptide is translocated into the lumen of the endoplasmic reticulum. The transfer of oligosaccharide precursor does not always proceed to completion; a given protein may be produced as a heterogeneous population with potential N-linked glycosylation sites variably occupied. Glycosylation site occupancy can vary with time during batch culture (Curling et al., 1990) and with changes in culture environment (Goochee and Monica, 1990). In order to produce product of consistent quality, it is desirable to understand the causes of this glycosylation site occupancy heterogeneity.

Detailed pathway alterations responsible for environmentally induced changes in glycosylation are often unknown. Factors believed to influence glycosylation site occupancy include availability of dolichol (Crick and Waechter, 1994;

Rosenwald et al., 1990), availability of nucleotide sugars (Rearick et al., 1981), activity of sugar transferase enzymes (Waldman et al., 1987), and variable glycosylation site accessiblity due to competition with protein folding (Allen et al., 1995; Holst et al., 1996; Shelikoff et al., 1996). One or more of these factors may be influenced by culture environment changes, leading to changes in heterogeneity. To further complicate matters, many changes in culture environment perturb normal cell function and metabolism, which may affect pathways involved in glycosylation. The relationship between central carbon metabolism and glycosylation is of particular interest. In this study we used metabolic flux analysis techniques to quantify central carbon metabolism to identify key reactions related to glycosylation site occupancy.

We studied the relationship between central carbon metabolism and glycosylation in a Chinese hamster ovary (CHO) cell line producing recombinant human interferon-γ (IFN-γ). IFN-γ has two potential N-linked glycosylation sites located at asparagine residues 25 and 97, and these sites are variably occupied leading to a mixture of proteins with either zero, one, or two glycosylation sites occupied (Rinderknecht et al., 1984; Sareneva et al., 1995). To determine how IFN-γ site occupancy is influenced by CHO cell metabolism, we performed a series of continuous culture (chemostat) experiments. Chemostat experiments are the preferred method for studying metabolic effects on glycosylation, because the accuracy of metabolite rate measurements is improved and cell physiology can be studied under well-defined, steady state conditions. Nutrient uptake and byproduct formation data were used to solve material balances for a biochemical network model of central carbon metabolism. From data obtained in glucose limited chemostats, we found that glycosylation site occupancy correlated with TCA cycle activity but not glycolytic activity. Site occupancy also correlated with intracellular nucleotide sugar concentrations. These findings led to the hypothesis that site occupancy was limited by nucleotide sugar formation, which was influenced primarily by nucleoside triphosphate availability. A glutamine limited chemostat illustrated that amino sugar formation can also limit the formation of the nucleotide sugar UDP-*N*-acetylglucosamine. Nucleotide and nucleotide sugar measurements from chemostat, batch, and fed-batch experiments confirmed that the primary determinants of UDP-sugar concentrations during exponential growth are UTP levels and amino sugar formation. During periods of glucose or glutamine starvation, nucleotide sugar availability can limit glycosylation site occupancy.

MATERIALS AND METHODS

Cell Line and Culture Medium

The Chinese hamster ovary cell line producing recombinant human gamma interferon (γ-CHO) was obtained from Dr. Walter Fiers at the University of Ghent, Belgium (Scahill et al., 1983). These cells were adapted to suspension growth in a serum free medium formulation developed at MIT. Designated RPMI-SFM, this medium uses RPMI-1640 as the base and is supplemented with Primatone RL (2.5 g/l), 2-hydroxypropyl-β-cyclodextrin (0.4 g/L), Pluronic F-68 (0.1% = 1 g/L), insulin (5 mg/L), transferrin (5 mg/L), trace elements (according to Hamilton and Ham (1977)), EDTA (6.3 mg/L), sodium pyruvate (1 m*M*), putrescine (1 μ*M*), choline chloride (11 mg/L), ethanolamine (100 μ*M*), linoleic acid (1.5 μ*M*), methotrexate (0.25 μ*M*), penicillin (100,000 units/L), and streptomycin (100 mg/L). For glucose limited continuous culture, glucose free RPMI-1640 was supplemented with 0.5 g/L glucose (2.78 m*M* = 25% of normal RPMI-1640), and glutamine was added to a final concentration of 0.45 g/L (3.08 m*M* = 150% of normal RPMI-1640). Similarly for glutamine limited chemostats, glutamine free RPMI-1640 was supplemented with 75 mg/L glutamine (0.51 m*M* = 25% of normal RPMI-1640) and 2.0 g/L glucose (11.11 m*M* = 100% of normal RPMI-1640). Primatone RL was obtained from Quest International (Norwich, NY) and all other components were obtained from Sigma (St. Louis, MO).

Batch and Fed-Batch Culture

Batch and fed-batch experiments were performed in 100 mL spinner flasks with an agitation rate of 80 rpm. Cultures were incubated at 37°C with a 5% CO_2 overlay. Batch cultures that were not run as controls for fed-batch experiments were inoculated at 2×10^5 cells/mL. Fed-batch cultures were inoculated at $(4–5) \times 10^5$ cells/mL in RPMI-SFM with 3 m*M* glucose and 0.5 m*M* glutamine. Feeding was performed with a stoichiometrically designed supplemental medium as described in Xie et al. (1997). Cell counts and feeding were performed every 12 h.

Uridine Fed Cultures

Uridine was added to designated cultures at final concentrations ranging from 1 to 10 m*M*. Cell growth and product formation were not affected over this range. Uridine (Sigma, St. Louis, MO) was added from a 100 m*M* stock solution prepared in RPMI-SFM. Cells were grown in 100 mL spinner flasks under conditions identical to those for normal batch and fed-batch cultures.

Continuous Culture and Material Balancing

Bioreactor operation, metabolite measurements and material balancing flux analysis were performed as described by Nyberg et al. (1998). Glucose limited steady states described here are identical to steady states 1–4 from Nyberg et al. (1998). Material balancing was based upon a metabolic network model of central carbon metabolism that included two redundant measurements. For consistent data sets, the final metabolic flux estimates were based upon a weighted least squares solution including all measurements. For the glucose limited steady state 1, the oxygen data was not included in the solution, because the data consistency analysis had identified the measurement as inconsistent (see

Nyberg et al. (1998) for a detailed discussion). Likewise, the oxygen and carbon dioxide data were not used in the weighted least squares solutions for the glucose limited steady state 3 and the glutamine limited steady state.

Analysis of Nucleotides and Nucleotide Sugars

Analysis of nucleotides and nucleotide sugars was performed based upon the methods of Ryll and Wagner (1991). Cells were extracted using perchloric acid (PCA), and neutralized extracts were analyzed with ion-pair reverse phase HPLC. Extracts were collected for glucose limited steady states 1, 2, and 4 and for the glutamine limited steady state (a cell extract was not performed for glucose limited steady state 3). Some modifications in the ion-pair HPLC buffers and gradients were required to obtain adequate separation of the desired nucleotides and nucleotide sugars.

Extraction of Cells

Approximately 5×10^6 cells were removed from the reactor and immediately centrifuged at 0°C and 190*g* for 3 min. After the supernatant was discarded, 500 μL of ice-cold 0.5 *M* perchloric acid (Mallinckrodt, Paris, KY) was added and the sample was vortexed vigorously. The sample was then placed on ice for 2 min before centrifuging at 4°C and 10,000*g* for 3 min. The supernatant was placed on ice, and the insoluble pellet was extracted a second time with 500 μL of ice-cold 0.5 *M* PCA. Following another centrifugation at 4°C and 10,000*g* for 3 min, the supernatants from the first and second extractions were combined. Eight-hundred μL of the combined extract was then neutralized with 200 μL of ice-cold 2.5 *M* KOH (Mallinckrodt) in 1.5 *M* K_2HPO_4 (Sigma, St. Louis, MO). After sitting on ice for 2 min, the neutralized sample was centrifuged at 4°C and 10,000*g* for 3 min to remove the potassium perchlorate precipitate. The supernatant was filtered using a 0.2 μm syringe filter (Acrodisc, Gelman Sciences, Ann Arbor, MI), and the samples were stored at –70°C prior to HPLC analysis.

Ion Pair High Performance Liquid Chromatography

In order to obtain acceptable separation of the desired nucleotides and nucleotide sugars from the cell extracts, we found it necessary to slightly modify the buffer pH's and gradients reported by Ryll and Wagner (1991). Two separate analyses with different buffer pH's and gradients were required to quantify all of the desired compounds. For both analyses the buffer compositions were the same: buffer A was 100 m*M* potassium phosphate buffer (Sigma) + 8 m*M* tetrabutylammonium hydrogen sulfate (Sigma), and buffer B was 70% buffer A plus 30% methanol (EM Science, Gibbstown, NJ). Buffers were prepared with HPLC grade water (EM Science) and were filtered (0.45 μm Durapore filter, Millipore, Bedford, MA) and degassed before use. Chromatography was performed using an HP 1090 HPLC (Hewlett Packard, Palo Alto, CA). Separation was achieved on a Supelcosil LC-18-T column (150 mm long × 4.6 mm inside diameter, 3 μm particle size) equipped with a guard column (Supelco, Bellefonte, PA). Sample detection by a diode array detector was at 254 nm, referenced to the 390 nm wavelength.

Nucleotide sugars and all nucleoside phosphates except UTP and GTP could be resolved using buffers A and B at pH = 6.0. Buffers were pH adjusted with 4 *M* phosphoric acid (Sigma) and 4 *M* KOH (Mallinckrodt). The gradient used was 0% buffer B for 7 min followed by a 0–40% buffer B linear gradient over 5 min, a 40–100% buffer B linear gradient over 6 min, a hold at 100% buffer B for 5 min, a switch from 100–0% buffer B in 1 min and finally a hold at 0% B for 6 min to equilibrate the column for the next sample. The flow rate was 1.5 mL/min, and the column temperature was controlled at 40°C. Figure 1 shows a typical chromatogram for a 150 μL injection of CHO cell perchloric acid extract analyzed using this method. Under these chromatographic conditions UTP and GTP co-eluted, but the two nucleotides could be resolved by switching to pH = 5.0 buffers. The nucleotide sugars UDP-glucose (UDP-Glc) and GDP-mannose (GDP-Man) also co-eluted, as did UDP-*N*-acetylglucosamine (UDP-GlcNAc) and UDP-*N*-acetylgalactosamine (UDP-GalNAc). These nucleotide sugars co-eluted under all conditions tested with PCA cell extracts, and so the composite UDP-Glc + GDP-Man and UDP-GNAc (UDP-GlcNAc + UDP-GalNAc) are reported here. UDP-GlcNAc and UDP-GalNAc can be intercon-

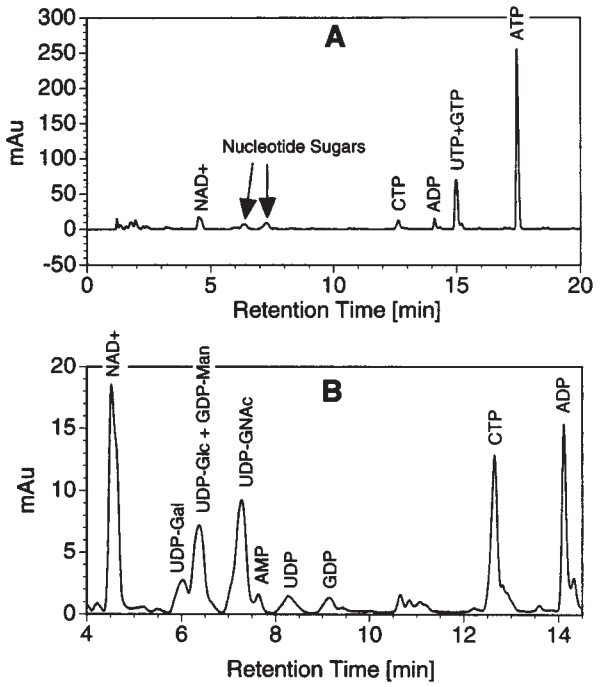

Figure 1. Sample chromatogram for a 150 μL injection of CHO cell PCA extract analyzed with pH = 6.0 buffers. (A) Entire chromatogram. (B) Detail of nucleotide sugar region.

verted readily by UDP-GalNAc 4-epimerase, and the two species were present at the equilibrium ratio in glucosamine fed HeLa cells (Kornfeld and Ginsburg, 1966). Therefore, the composite UDP-GNAc is expected to indicate relative UDP-GlcNAc abundance. UDP-GlcNAc is the more relevant nucleotide sugar for this analysis, since GlcNAc is incorporated into the precursor oligosaccharide in N-glycosylation. GalNAc, in comparison, is not normally incorporated into N-linked glycans.

Switching buffers A and B to pH = 5.0 provided resolution between UTP and GTP, but the retention times of UDP and GDP also shifted. When PCA cell extracts were analyzed, the UDP and GDP peaks overlapped with nucleotide sugar peaks to such an extent that they were difficult to quantify. For this reason samples were run with pH = 6.0 buffers to quantify all nucleotide sugars and nucleotides except for UTP and GTP. At a pH of 5.0, it was possible to quantify UTP and GTP and to obtain additional measurements for ATP, ADP, and CTP. The gradient used with pH = 5.0 buffers was a 0–25% buffer B linear gradient over the first 22.5 min followed by a 25–100% buffer B linear gradient over 3.5 min, a hold at 100% buffer B for 6 min, a switch from 100–0% buffer B in 1 min, and finally a hold at 0% buffer B for 7 min to equilibrate the column for the next sample. The flow rate was 1.5 mL/min, and the column temperature was set at 40°C. Figure 2 shows a typical chromatogram for a 150 μL injection of CHO cell PCA extract analyzed with pH 5.0 buffers.

Chromatogram peaks were identified by comparing retention times and by analyzing samples spiked with standards (nucleotide and nucleotide sugar standards were obtained from Sigma), and these results agreed with the elution order and peak designations reported by Ryll and Wagner (1991). Integrated peak areas were used for quantification. Peak areas were related to concentration via standard curves which were obtained by running standards at concentrations between 100 and 10,000 pmol. Concentration was linearly related to peak area over this range.

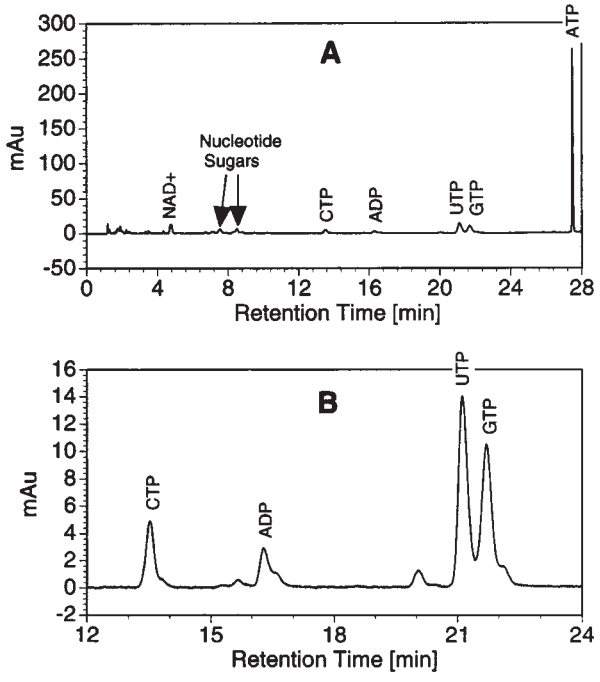

Figure 2. Sample chromatogram for a 150 μL injection of CHO cell PCA extract analyzed with pH = 5.0 buffers. (A) Entire chromatogram. (B) Detail of UTP and GTP separation.

Analysis of Glycosylation Site Occupancy Heterogeneity

Glycosylation site occupancy heterogeneity was analyzed by immunoprecipitating IFN-γ from culture supernatants and analyzing the purified product using micellar electrokinetic capillary chromatography (MECC). Following immunoprecipitation, the IFN-γ was directly eluted into the MECC running buffer. This procedure provided more reproducible glycosylation site occupancy results than when IFN-γ was purified with affinity chromatography followed by a low pH (pH = 2–3) elution. Purifications that involved a low pH elution yielded nonreproducible fractions of nonglycosylated protein (data not shown). Nonglycosylated γ-interferon is known to unfold at low pH and aggregate in the presence of salts. This aggregation has been suggested as the reason IFN-γ activity is unstable in an acid environment (Arakawa and Hsu, 1987). Furthermore the Asn-25 glycan of glycosylated IFN-γ has been shown to play an important role in folding and dimerization (Sareneva et al., 1994). We hypothesize that nonreproducible results obtained using low pH elution may have been due to aggregation of nonglycosylated IFN-γ, while the glycans of glycosylated IFN-γ may have prevented or reduced aggregation loss.

Immunoprecipitation

Samples containing approximately 10 μg of IFN-γ (between 4 and 8 mL of chemostat steady state samples) were filtered (0.22 μm Millex-GV, Millipore, Bedford, MA) and mixed 2:1 with IP reaction buffer (50 m*M* Tris-HCl, 5 m*M* EDTA, 5 m*M* EGTA, pH = 8.2). Thirty-five μL of a 1:1 suspension of phosphate buffered saline:IgG antibody (anti-IFN-γ)-Sepharose complex (Reselute-γ, Celltech Ltd., Slough, UK) was added to each sample. Samples were incubated at 4°C with agitation overnight. Following incubation samples were centrifuged for 1 min at 200*g*, and the pellet was washed twice with wash buffer I (0.5% Nonidet P40, 50 m*M* Tris-HCl, 500 m*M* NaCl, 5 m*M* EDTA, 1 g/L bovine serum albumin, pH = 8.0), twice with wash buffer II (0.5% Nonidet P40, 50 m*M* tris-HCl, 5 m*M* EDTA, pH = 8.0), and once with water. Samples were eluted directly into 35 μL of filtered (0.45 μm Durapore filter, Millipore), degassed MECC running buffer (20 m*M* sodium borate, 20 m*M* boric acid, 100 m*M* SDS, pH = 8.2). The samples were incubated at room temperature for 5 min after adding the MECC running buffer, then vortexed, and centrifuged for 1

min at 200*g*, and the supernatants were transferred to 0.5 mL microcentrifuge tubes for MECC analysis. All buffer components were from Sigma (St. Louis, MO).

Micellar Electrokinetic Capillary Chromatography

The immunoprecipitated IFN-γ was analyzed using MECC based upon the method described by James et al. (1994). An analytical capillary electrophoresis system (Model 270A, Applied Biosystems, Foster City, CA) was equipped with a 75 μm inside diameter × 70 cm long (50 cm to detector) neutral hydrophilic bonded silica capillary (CElect P175, Supelco, Bellefonte, PA). New capillaries were conditioned by washing with 0.1 *M* KOH (Mallinckrodt) for 10 min, followed by 1 h of MECC running buffer. Between each separation the capillary was rinsed with 0.1 *M* KOH for 2 min and then MECC running buffer for 5 min. Samples were vacuum injected over 3 s, and then a 17 kV voltage was applied to the capillary. The separation was performed at 30°C, and the detection wavelength was set to 200 nm. The separate peaks for 2-site, 1-site, and nonglycosylated IFN-γ eluted within 25 min, with glycoform migration time inversely related to extent of glycosylation as shown in Fig. 3. Chromatograms were exported from the System Gold software used for data acquisition (Beckman Instruments, Fullerton, CA) and were analyzed using the GS370 peak integration software (Version 3.0, Hoefer Scientific Instruments, San Francisco, CA).

RESULTS

Glycosylation Site Occupancy in Continuous Culture

Glycosylation site occupancy heterogeneity was monitored in one glutamine limited and four glucose limited chemostat cultures. Dilution rates ranged from 0.0125 to 0.0248 1/h, which represents a range of 38% to 75% of the typical maximum growth rate observed in batch culture (batch culture $\mu_{max} \sim 0.033$ 1/h). Significant cell death was observed at low dilution rates, and this death increased as the dilution decreased. Since only viable cells can divide, the growth rate can deviate significantly from the dilution rate at low dilutions ($\mu = D$/viability). Increasing death with decreasing dilution rate has been observed before with CHO cell chemostats (Hayter et al., 1993).

Glycosylation site occupancy at these steady states was analyzed using micellar electrokinetic capillary chromatography (MECC) of immunoprecipitated samples, and the results are presented in Table I. Immunoprecipitations were performed in duplicate, and each immunoprecipitated sample was injected 2–3 times in MECC. Although growth rates and viabilities varied significantly at the different steady states, glycosylation site occupancy was found to vary over a rather narrow range. No obvious correlations were evident between site occupancy and growth rate.

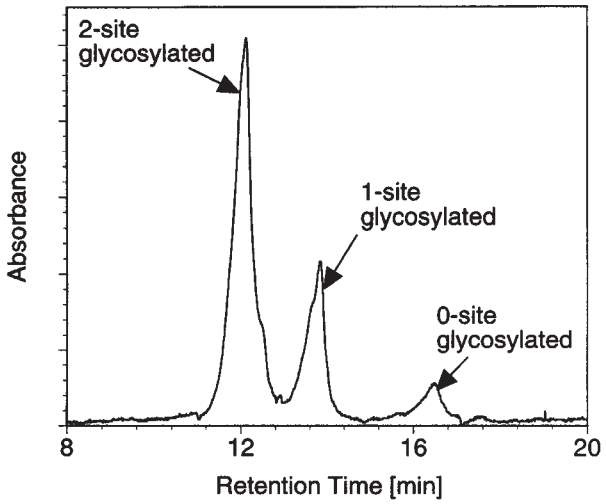

Figure 3. Capillary electrophoresis resolution of 2-site, 1-site, and 0-site glycosylated IFN-γ.

Glycosylation Site Occupancy and Nucleotide Sugars

Nucleotide sugar concentrations were analyzed to determine whether their availability was responsible for the observed variations in glycosylation site occupancy. Perchloric acid cell extracts were collected for the glutamine limited chemostat and for three of the four glucose limited chemostats, and the extracts were analyzed with ion-pair reverse phase HPLC as described in Materials and Methods. The measured nucleotide concentrations are reported in Table II as μmol/(g viable dry cell weight). Results are expressed on a dry cell weight rather than cell number basis to account for variations in cell size and because extensive cell aggregation (clumping) at low dilution rates made cell number determination difficult (Nyberg et al., 1998). Perchloric acid extracts of nonviable (trypan blue permeable) cells were found to contain negligible concentrations of nucleotides and nucleotide sugars (data not shown). This result was not surprising, since loss of membrane integrity, as measured by trypan blue permeability, was expected to increase free nucleotide permeability. Hence, nucleotide concentration results are considered on a viable dry cell weight basis.

Table I. Glycosylation site occupancy for four glucose limited and one glutamine limited steady state cultures.

	Dilution rate, D (1/h)	Growth rate, μ (1/h)	Glycosylation sites occupied (%)		
			2 sites	1 sites	0 sites
Glucose-limited 1	0.0227	0.0238	69.8 ± 1.1	25.1 ± 0.4	5.0 ± 0.8
Glucose-limited 2	0.0176	0.0186	66.3 ± 0.4	26.9 ± 0.2	6.7 ± 0.2
Glucose-limited 3	0.0141	0.0163	68.3 ± 0.8	25.0 ± 0.6	6.6 ± 0.6
Glucose-limited 4	0.0125	0.0165	65.2 ± 1.2	28.0 ± 1.0	6.7 ± 0.8
Glutamine-limited	0.0248	0.0254	61.7 ± 0.8	30.0 ± 0.6	8.2 ± 0.4

Table II. Cell mass-specific nucleotide concentrations (μmol/g viable dry cell weight) measured in perchloric acid extracts. A perchloric acid extract was not collected for glucose limited steady state 3.

Nucleotide	Glucose limited 1	Glucose limited 2	Glucose limited 4	Glutamine limited
ATP	25.40 ± 0.19	21.68 ± 0.25	19.18 ± 0.43	25.07 ± 0.37
ADP	2.57 ± 0.36	2.18 ± 0.14	2.09 ± 0.27	1.58 ± 0.10
AMP	0.49 ± 0.03	0.43 ± 0.03	0.49 ± 0.06	0.25 ± 0.02
GTP	4.62 ± 0.07	3.96 ± 0.03	3.57 ± 0.07	4.87 ± 0.06
GDP	0.54 ± 0.06	0.41 ± 0.01	0.50 ± 0.08	0.31 ± 0.04
CTP	3.79 ± 0.19	3.34 ± 0.01	2.82 ± 0.06	4.17 ± 0.11
UTP	7.81 ± 0.21	6.72 ± 0.01	4.87 ± 0.05	9.66 ± 0.05
UDP	0.75 ± 0.19	0.56 ± 0.03	0.63 ± 0.11	0.82 ± 0.04
UDP-Gal	0.64 ± 0.33	0.66 ± 0.16	0.50 ± 0.10	1.10 ± 0.03
UDP-Glc + GDP-Man	2.16 ± 0.20	2.05 ± 0.06	2.00 ± 0.15	2.57 ± 0.12
UDP-GNAc	2.85 ± 0.02	2.30 ± 0.08	1.98 ± 0.08	1.70 ± 0.02

As the glycosylation site occupancy decreased, there was a corresponding decrease in intracellular UDP-*N*-acetylglucosamine + UDP-*N*-acetylgalactosamine (the nucleotide sugars co-eluted in HPLC as discussed in Materials and Methods; the sum will be referred to as UDP-GNAc). Figure 4 shows the percentage of IFN-γ glycosylated at both potential sites against the intracellular UDP-GNAc. A trend, consistent for all of the glucose and glutamine limited chemostats, is identified. For the glucose limited chemostats, the concentrations of all nucleotides and nucleotide sugars declined as UDP-GNAc declined, indicating that declining UDP-GNAc may have been related to an overall reduction in nucleotide levels. UDP-Glucose and GDP-Mannose, the other nucleotide sugars involved in the initial steps of N-linked glycosylation, may have also declined as site occupancy decreased in glucose limited cultures; however, because of experimental uncertainty in the measured UDP-Glucose + GDP-Mannose values (the nucleotide sugars co-eluted in HPLC as discussed in Materials and Methods), conclusions cannot be drawn concerning these nucleotide sugars. In contrast to the glucose limited cultures, the glutamine limited culture had high levels of nucleoside triphosphates and UDP-Glucose + GDP-Mannose but very low UDP-GNAc.

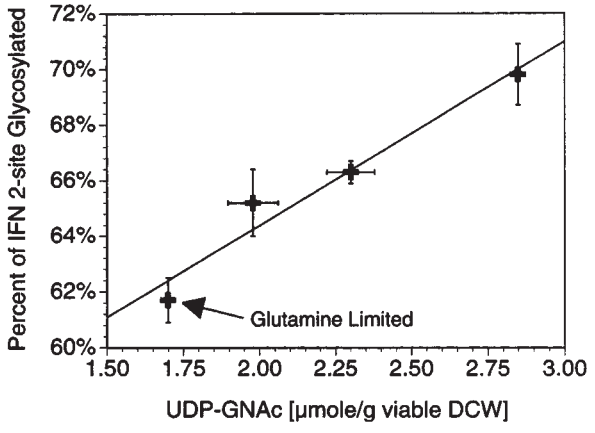

Figure 4. The relationship between glycosylation site occupancy and intracellular UDP-GNAc concentration in glucose and glutamine limited chemostat cultures.

Reaction Yields Correlated with Glycosylation Site Occupancy

To determine whether changes in nucleotide sugars and glycosylation were related to metabolism, the fluxes of central carbon metabolism were estimated from material balances. Figure 5 depicts the metabolic network model used (Nyberg et al., 1998). Estimates of intracellular fluxes obtained by material balancing are presented in Table III. Fluxes were normalized by the growth rate, μ, instead of the uptake rate of a particular nutrient to facilitate comparisons of flux distributions at different steady states and nutrient limitations. Normalizing by the growth rate allows direct comparison of the reaction yields (mmol/g dry cell weight), which are measures of reaction pathway activities per cell mass produced.

For the glucose limited chemostats, glycosylation site occupancy correlated strongly with citric acid (TCA) cycle activity. The percentage of IFN-γ glycosylated at both potential sites was linearly related to TCA cycle reaction yields. Figure 6 shows these relationships for the pyruvate-to-acetyl CoA reaction (R^2 = 0.997), the α-ketoglutarate-to-succinyl CoA reaction (R^2 = 0.990), and the oxaloacetate-to-α-ketoglutarate reaction (R^2 = 0.965). In contrast, no correlation was observed between glycosylation site occupancy and the reactions of glycolysis (see Table III, reactions 1, 2, and 3). This was somewhat surprising, since the hexose donor in nucleotide sugar formation is derived from isomerization of glucose-6-P, an intermediate in glycolysis.

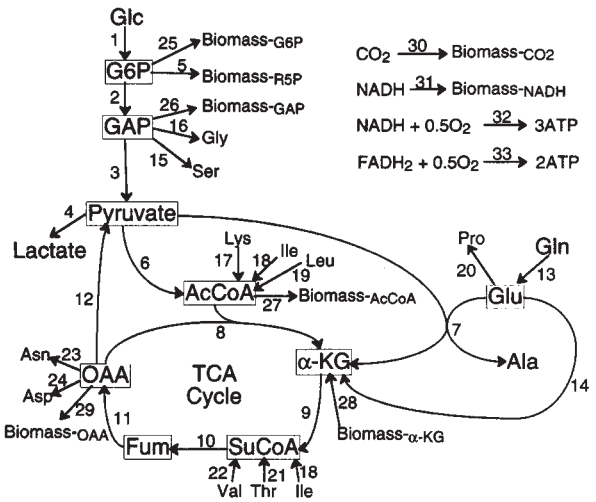

Figure 5. Schematic diagram of a simplified biochemical reaction network describing central carbon metabolism.

Table III. Estimated central carbon metabolism reaction yields (mmol/g viable dry cell weight) for four glucose limited and one glutamine limited steady state cultures. A complete listing of all reactions including cometabolites can be found in Nyberg et al. (1998).

	Reaction	Glucose limited 1	Glucose limited 2	Glucose limited 3	Glucose limited 4	Glutamine limited
1	Glc → G6P	4.96	4.05	3.80	4.26	13.67
2	G6P → 2 GAP	4.52	3.62	3.37	3.82	13.24
3	GAP → Pyr	7.98	6.42	5.56	6.23	26.22
4	Pry → Lac	1.89	0.51	0.11	–0.27	15.44
5	G6P → Biomass_R5P + CO_2	0.19	0.19	0.19	0.19	0.19
6	Pyr → AcCoA + CO_2	9.53	11.50	10.37	11.95	12.55
7	Pyr → Glu ↔ α-KG + Ala	0.95	–0.41	–0.47	–0.75	0.12
8	Oaa → AcCoA → α-KG + CO_2	6.03	9.24	8.17	10.68	10.33
9	α-KG → SuCoA + CO_2	10.02	13.40	11.88	14.58	11.18
10	SuCoA → Fum	10.05	13.85	12.08	14.79	11.55
11	Fum → Oaa	10.05	13.85	12.08	14.79	11.55
12	Oaa → Pyr + CO_2	4.38	5.18	4.44	4.70	1.89
13	Gln → Glu	4.67	4.51	4.33	4.60	0.50
14	Glu → α-KG	2.31	4.29	3.50	3.78	1.12
15	GAP + Glu → Ser + α-KG	0.66	0.45	0.46	0.49	0.11
16	GAP + Glu → Gly + α-KG	0.17	0.15	0.49	0.70	–0.09
17	Lys → 2 AcCoA + 2 CO_2	–0.05	–0.14	0.04	0.30	0.07
18	Ile → AcCoA + SuCoA	0.11	0.25	0.19	0.23	0.22
19	Leu → 3 AcCoA	0.27	0.69	0.61	0.73	0.57
20	Glu → Pro	0.49	0.20	0.12	0.08	0.03
21	Thr → SuCoA	–0.09	–0.10	–0.19	–0.26	–0.06
22	Val → SuCoA + CO_2	0.01	0.29	0.20	0.24	0.21
23	Oaa + Gln → Asn + α-KG	–0.45	–0.54	–0.62	–0.65	–0.44
24	Oaa + Glu → Asp + α-KG	0.00	–0.13	0.00	–0.03	–0.32
25	G6P → Biomass_G6P	0.25	0.25	0.25	0.25	0.25
26	GAP → Biomass_GAP	0.23	0.23	0.23	0.23	0.23
27	AcCoA → Biomass_AcCoA	4.31	4.29	4.30	4.28	4.30
28	Biomass_AKG → α-KG	0.35	0.35	0.35	0.35	0.35
29	Oaa → Biomass_OAA	0.09	0.09	0.09	0.09	0.09
30	CO_2 → Biomass_CO_2	–0.22	–0.22	–0.22	–0.22	–0.22
31	NADH → Biomass_NADH	5.38	5.38	5.38	5.37	5.38
32	0.5 O_2 + 3 ADP + NADH → 3 ATP + NAD^+	40.40	56.32	50.43	63.56	55.09
33	0.5 O_2 + 2 ADP + $FADH_2$ → 2 ATP + FAD	10.39	14.94	13.12	16.29	12.63

The results suggest that hexose availability was not the limiting factor for nucleotide sugar formation.

Nucleoside Triphosphates and Nucleotide Sugars from Chemostat Cultures

The correlation between glycosylation and the TCA cycle implicates nucleoside triphosphates as the main factor influencing nucleotide sugar levels. The reactions of the TCA cycle impact nucleotide synthesis, because potential TCA metabolites, such as aspartate and glutamine, are important intermediates in pyrimidine and purine base synthesis (Stryer, 1988). When the TCA cycle is producing more energy and fewer byproducts, the yield of TCA cycle reactions increases and nucleotide synthesis declines. In such cases available carbon is used to generate energy, and less carbon is available for biosynthesis. The observation from the glucose limited chemostats that declining nucleotide sugars correlated with declining total nucleotide levels supports the hypothesis that nucleoside triphosphate levels

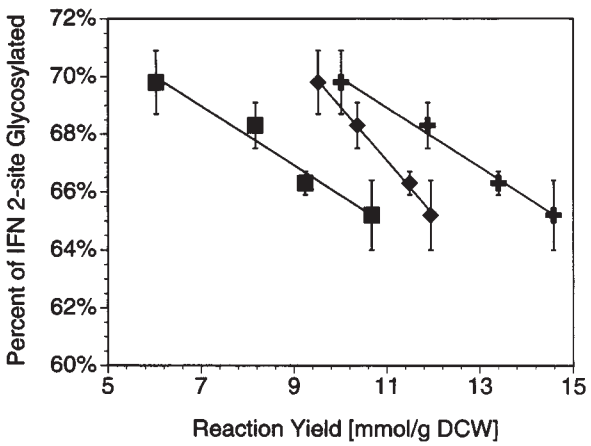

Figure 6. Reaction yields correlated to glycosylation site occupancy heterogeneity in glucose limited chemostat cultures. Site occupancy correlated with the yield of the pyruvate to acetyl CoA reaction (◆) and the reactions of the TCA cycle such as oxaloacetate-to-α-ketoglutarate (■) and α-ketoglutarate-to-succinyl CoA (✚).

were impacting nucleotide sugar concentrations. Figure 7 shows the relationship between UDP-GNAc and UTP. For glucose limited chemostats, UDP-GNAc levels declined as UTP declined.

It is noted that the glutamine limited chemostat did not follow the same trends regarding TCA cycle activity, nucleoside triphosphates and nucleotide sugars. Although glycosylation site occupancy in the glutamine limited chemostat did correlate with UDP-GNAc, the low levels of UDP-GNAc did not appear to be related to UTP concentration or the TCA cycle. The UTP concentration was much higher relative to the UDP-GNAc level for the glutamine limited culture (Fig. 7). A possible cause of the low UDP-GNAc concentration in this case is limitation of the *N*-acetylglucosamine-1-P precursor. The committed step in the formation of this amino sugar is conversion of fructose-6-P to glucosamine-6-P, which is normally catalyzed by the enzyme glutamine:fructose-6-P amidotransferase (GFAT). GFAT uses glutamine as an ammonia donor, and hence glutamine limitation would be expected to inhibit amino sugar synthesis. There is evidence that when ammonia concentrations are high, ammonia can also be used directly for amino sugar formation (Ryll et al., 1994). The ammonia concentration in the glutamine limited chemostat was lower than the concentrations in any of the glucose limited chemostats (see Table IV), and therefore ammonia was also less available for amino sugar formation. For the glucose limited chemostats, UDP-GNAc concentrations did not correlate with glutamine or ammonia concentrations. The data are consistent with the hypothesis that amino sugar formation was not limiting UDP-GNAc formation in the glucose limited chemostats.

Nucleoside Triphosphates and Nucleotide Sugars from Batch and Fed-Batch Cultures

Examination of nucleotide levels in batch and fed-batch cultures supports the hypothesis that nucleoside triphosphates are the primary determinants of nucleotide sugar concentrations in the absence of glutamine limitation. Figure 8 shows UDP-GNAc vs. UTP during exponential growth in batch, fed-batch and chemostat cultures. Intracellular UTP levels varied between 5 and 10 μmol/g viable dry cell weight over the course of fed-batch cultures. Higher concentrations of UTP were obtained by feeding the nucleotide precursor uridine (up to 10 m*M*), while lower concentrations were observed during glucose starvation at the end of batch culture. Figure 8 demonstrates that UDP-GNAc was linearly correlated with UTP over a 10-fold range in UTP (from 2.5 to 25 μmol/g vDCW). Similar correlations were found for UDP-Gal and UDP-Glc (data not shown), indicating that in general UDP-sugar levels are regulated by nucleoside triphosphate concentrations. This data is in agreement with the data of Pels Rijcken et al. (1995), who found that rat hepatocytes fed 0.5 m*M* uridine for 40 h increased the pools of UTP, UDP-hexose, and UDP-GNAc 6.7-, 3.8-, and 4.6-fold, respectively.

Nucleotide triphosphates are not the only regulators of UDP-sugar synthesis, however, as the glutamine limited chemostat demonstrates. In this case amino sugar formation appears to limit UDP-GNAc synthesis. Figure 9 re-plots the data from Figure 8 along with additional data from glutamine limited cultures (the glutamine limited chemostat and cells starved for glutamine in batch and fed-batch culture). The data from glutamine limited cultures fall below the exponential growth data, indicating an excess of UTP com-

Table IV. Steady state ammonia concentrations (m*M*) in glucose limited and glutamine limited chemostat cultures.

	Glucose limited 1	Glucose limited 2	Glucose limited 3	Glucose limited 4	Glutamine limited
Ammonia	4.47	5.64	5.84	5.95	1.71

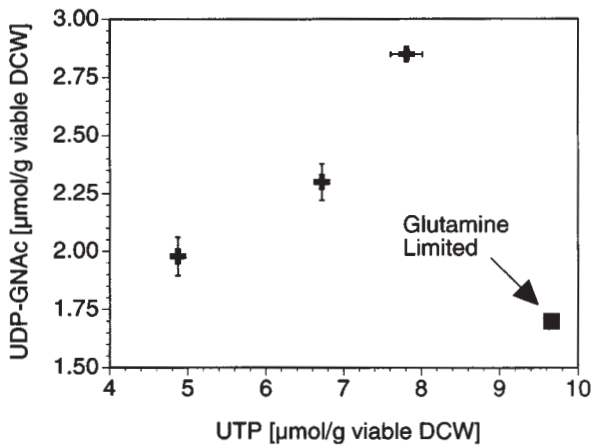

Figure 7. The relationship between intracellular UDP-GNAc concentration and UTP in glucose and glutamine limited chemostat cultures.

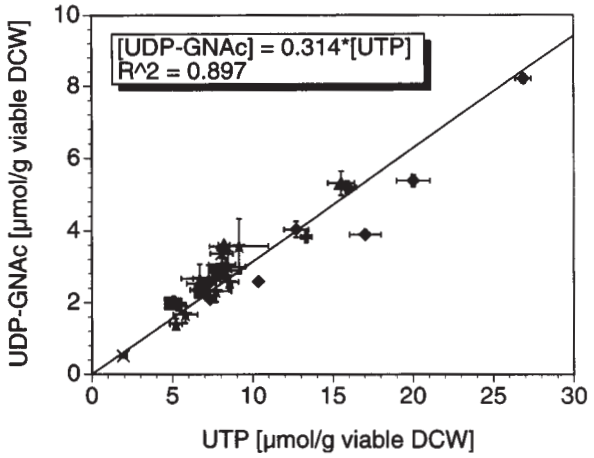

Figure 8. The correlation between intracellular UDP-GNAc and UTP during exponential growth in batch, fed-batch, and chemostat cultures. Symbols indicate results from various independent experiments.

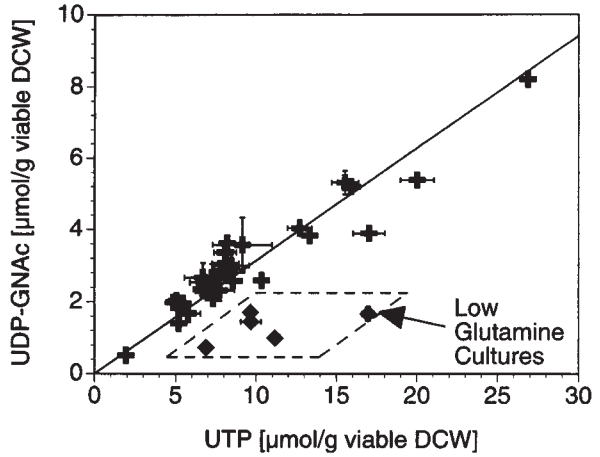

Figure 9. Reduced UDP-GNAc formation under glutamine limitation: the relationship between UDP-GNAc and UTP during glutamine limitation (◆) compared to exponential growth in batch, fed-batch, and chemostat cultures (✚).

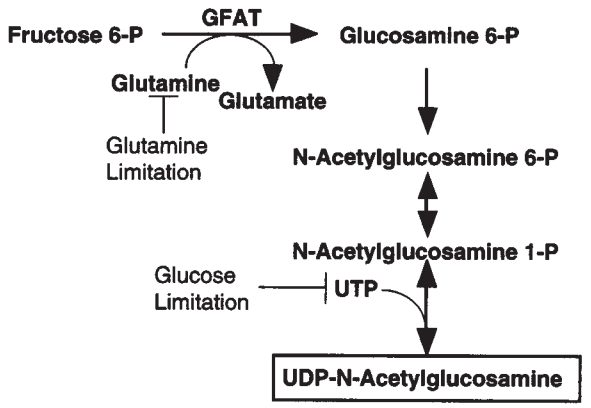

Figure 10. Synthesis of UDP-GlcNAc under glucose and glutamine limitation. During glucose starvation, nucleoside triphosphates including UTP are depleted, which limits nucleotide sugar formation. In contrast, glutamine starvation limits UDP-GlcNAc synthesis by preventing amino sugar formation.

pared to UDP-GNAc. The glutamine starvation effect was specific to amino sugars, since UDP-Glc and UDP-Gal still correlated with UTP (data not shown). Thus amino sugar formation most likely limits UDP-GNAc synthesis during glutamine starvation.

DISCUSSION

In this paper we studied glycosylation site occupancy of recombinant IFN-γ in continuous culture of Chinese hamster ovary cells. We found that site occupancy varied with intracellular UDP-GNAc (the combined UDP-GlcNAc and UDP-GalNAc pool) for the glucose and glutamine limited steady states analyzed. Based upon analysis of nucleotide levels and estimates of central carbon metabolic fluxes, we propose the model in Fig. 10 to explain the effects of glucose and glutamine limitation. During glucose limitation available carbon is preferentially used for energy production, causing reduced nucleotide biosynthesis. Because they are continually consumed for RNA synthesis, nucleoside triphosphates such as UTP become depleted. Lower nucleoside triphosphate pools in turn cause lower nucleotide sugar pools and lower glycosylation site occupancy. During glutamine deprivation, amino sugar formation limits UDP-GNAc synthesis, since glutamine is the ammonia donor in this reaction.

While it has been known for some time that glucose starvation decreases glycosylation efficiency (Baumann and Jahreis, 1983; Chapman and Calhoun, 1988; Gershman and Robbins, 1981; Rearick et al., 1981; Stark and Heath, 1979; Turco, 1980), the exact mechanism of this effect has remained unresolved. Glucose starved cells synthesize truncated lipid-linked oligosaccharide precursors, which are transferred to protein with a lower efficiency than the normal precursor (Chapman and Calhoun, 1988; Gershman and Robbins, 1981; Rearick et al., 1981). Nucleotide sugar depletion has also been observed in glucose starved cultures (Chapman and Calhoun, 1988; Ullrey and Kalckar, 1979), and it is often cited as the likely cause of truncated precursor synthesis. Proposed explanations for nucleotide sugar depletion during glucose starvation have generally focused on supply of hexose phosphates, but little work has been done to investigate these hypotheses. In this paper we present evidence that nucleoside triphosphate depletion is the cause of reduced nucleotide sugar concentrations during glucose starvation.

Evidence from the literature supports our hypothesis that glucose starvation affects glycosylation by causing depletion of nucleoside triphosphates. Nucleoside triphosphate depletion during glucose starvation has been observed in the past (Kaminskas, 1979; Rapaport et al., 1979). Declines in nucleoside triphosphates were not explained by increases in nucleoside mono- and diphosphates, indicating that the nucleosides were being depleted. Treatment with cycloheximide, which inhibits protein and RNA synthesis, was found to prevent the decline in ribonucleotide pools during glucose starvation. This result suggests that RNA synthesis plays a role in ribonucleotide depletion during glucose starvation. Interestingly, other experiments have shown that cycloheximide treatment allows glucose starved cells to synthesize the normal $Glc_3Man_9GlcNAc_2$-P-P-Dol precursor oligosaccharide (Chapman and Calhoun, 1988). Hence under glucose starved conditions which do not lead to depletion of nucleoside triphosphates, glycosylation appears normal. This may also explain the results of Lanks et al. (1988), who found that feeding nucleosides was more effective on a molar basis than feeding glucose to suppress glucose regulated protein synthesis in glucose starved murine L929 cells. When glycosylation efficiency is impaired, synthesis of glucose regulated proteins such as BiP (GRP78) is induced, presumably because the underglycosylated proteins misfold and accumulate (Kozutsumi et al., 1988; Lee, 1987;

Wooden et al., 1991). The finding that uridine feeding can suppress GRP synthesis in glucose starved cultures strongly suggests that uridine fed cells are able to maintain normal glycosylation patterns.

For the glucose limited chemostat experiments described here, nucleotide concentrations appeared to vary in response to changes in metabolism. The reactions of the citric acid (TCA) cycle in particular were found to correlate with nucleotide levels and glycosylation in glucose limited chemostats (see Fig. 6). Metabolism could impact nucleotide biosynthesis by altering the availability of important precursor metabolites such as aspartate, glutamine, serine, glycine, and ribose-5-P. Of these precursor metabolites, the TCA cycle is most likely to impact aspartate. The importance of the TCA cycle in providing aspartate for nucleotide synthesis was demonstrated in a respiration deficient Chinese hamster lung fibroblast cell line which had an almost complete shutdown of TCA cycle reactions (DeFrancesco et al., 1976). While the cells were able to grow when 3 m*M* asparagine was added to the medium, the amount of ^{14}C labeled ATP was reduced by 70% compared to control cells, and UDP-glucose was reduced by 50%. Exogenous aspartate would not even support growth, apparently because it was less readily taken up by the cells. The data suggest that exogenous asparagine can only partially satisfy the demand for intracellular aspartate, and normal nucleotide synthesis relies on the TCA cycle for aspartate supply.

Aspartate is synthesized by the enzyme aspartate aminotransferase, which catalyzes the transfer of a glutamine ammonia group to oxaloacetate. Oxaloacetate is a TCA cycle intermediate which can also react with acetyl CoA to form citrate by the citrate synthase enzyme. Eigenbrodt et al. (1985) cited evidence that oxaloacetate availability is a primary regulator of aspartate formation, and the citrate synthase and aspartate aminotransferase reactions can compete for available oxaloacetate. High concentrations of acetyl CoA favor consumption of oxaloacetate for citrate synthesis, and so increased pyruvate oxidation leads to consumption of oxaloacetate in the TCA cycle and lower aspartate production. Interestingly, we found that increased pyruvate oxidation in glucose limited chemostats led to lower glycosylation site occupancy (Fig. 6). Thus when carbon utilization patterns favored consumption of oxaloacetate for citrate synthesis, nucleotide levels and glycosylation site occupancy declined. The data are consistent with the hypothesis that oxaloacetate availability for aspartate synthesis influenced nucleotide synthesis, which in turn influenced nucleotide sugars and glycosylation site occupancy. Glycosylation was best when pyruvate was converted to byproducts such as lactate and alanine, while the worst glycosylation occurred when both lactate and alanine were consumed and more pyruvate was oxidized.

The glutamine limited chemostat demonstrated that, although nucleoside triphosphates play an important role in determining nucleotide sugar concentrations, they are clearly not the only factor. Amino sugar formation can also determine the supply of UDP-GNAc. The glutamine:fructose-6-P amidotransferase (GFAT) enzyme responsible for amino sugar formation transfers an ammonia group from glutamine to fructose-6-P to form glucosamine-6-P. The rate of this reaction depends upon the concentration of glutamine and fructose-6-P, among other factors. Traxinger and Marshall (1991) reported GFAT's glutamine K_m values measured in adipose, liver, and other tissues ranged from 0.4 to 1.6 m*M*. The steady-state concentration of glutamine in the glutamine limited chemostat was 0.022 m*M*. While the intracellular glutamine concentration most likely differed from the extracellular concentration, one would expect intracellular glutamine was in short supply as well. Limited glutamine supply for amino sugar formation could explain low UDP-GNAc and high UTP concentrations under glutamine limitation (Fig. 9).

Further evidence implicating amino sugar formation as a regulator of UDP-GNAc synthesis is that feeding amino sugars such as glucosamine or galactosamine leads to accumulation of UDP-GNAc (Kornfeld and Ginsburg, 1966; Pels Rijcken et al., 1995). Following their entry into the cell, amino sugars are converted into hexosamine phosphates, acetylated, and reacted with UTP to make UDP-GNAc. Since the reaction catalyzed by GFAT is normally not reversible, glucosamine-6-P is not converted to fructose-6-P, and the majority of the hexosamine accumulates as nucleotide sugars. UDP-GNAc accumulation is also observed during exposure of cultured cells to high concentrations of ammonia (Ryll et al., 1994). When ammonia levels are elevated, the reverse of the glucosamine-6-P deaminase reaction can form glucosamine-6-P from fructose-6-P and ammonium. Excessive amino sugar formation leads to accumulation of UDP-GNAc. Accumulation of UDP-GNAc during exposure to amino sugars or elevated ammonia concentrations demonstrates that amino sugar formation can play a key role in regulating UDP-GNAc synthesis. Under normal conditions amino sugar formation must be tightly regulated to maintain sufficient supply of glucosamine-6-P, without overstimulating nucleotide sugar formation.

Exposure to ammonia or amino sugars is known to affect protein glycosylation, but the role that UDP-GNAc plays in mediating these effects is unclear. For example, both glucosamine and galactosamine cause similar accumulation of UDP-GNAc, but the two amino sugars impact glycosylation quite differently. Glucosamine feeding causes a reduction in glycosylation (Datema and Schwarz, 1979; Elbein, 1987; Koch et al., 1979; Pan and Elbein, 1982), while rat hepatocytes fed galactosamine slightly increased mannosylation of proteins and increased sialylation by a factor of 2.5 (Pels Rijcken et al., 1995). Moreover, 5 m*M* glucosamine caused truncated precursor oligosaccharide synthesis in MDKC cells, while the same concentration of galactosamine did not influence precursor synthesis or glycosylation (Pan and Elbein, 1982). Koch et al. (1979) suggest that the negative impact of glucosamine on glycosylation might be due to glucosamine itself rather than a nucleotide sugar, since reversibility of the glucosamine effect correlated with glucosamine during a period when UDP-Glc, UDP-GlcNAc, and

GDP-Man did not change significantly. Likewise, ammonia has been shown to impact glycosylation by altering sialylation (Anderson and Goochee, 1995; Gawlitzek et al., 1995; Kopp et al., 1995; Thorens and Vassalli, 1986), branching (Gawlitzek et al., 1995), and site occupancy (Borys et al., 1994), but it is not clear whether the effects are due to changes in intracellular pH (Anderson and Goochee, 1995) or to alterations in UDP-GNAc (Ryll et al., 1994). In this study we present evidence that depletion of UDP-GlcNAc (as a result of either nucleoside triphosphate or amino sugar limitation) can influence glycosylation site occupancy.

CONCLUSIONS

Continuous culture experiments allowed us to analyze central carbon metabolism under conditions which led to varied product glycosylation site occupancy. Although site occupancy varied over a narrow range, we found that differences correlated with the intracellular UDP-GNAc concentration. Measured nucleotide levels and estimates of central carbon metabolic fluxes point to nucleotide triphosphate depletion as the cause of decreased site occupancy during glucose limitation. Subsequent experiments in batch and fed-batch culture have confirmed that UDP-sugar concentrations are correlated with UTP levels in the absence of glutamine limitation. Glutamine limitation appears to influence glycosylation by reducing amino sugar formation and hence UDP-GNAc concentrations.

It should be emphasized that continuous culture experiments are used to study cells under nutrient limitation. We found that under glucose or glutamine limitation, nucleotide sugar formation can be responsible for observed changes in glycosylation site occupancy. Under nonlimiting conditions, nucleotide sugars may or may not play an important role in regulating glycosylation site occupancy. The relatively modest change in site occupancy (from 70% to 62% 2-site glycosylated protein) for a 40% reduction in UDP-GNAc tends to suggest that nucleotide sugar concentrations can vary over a fairly wide range without having major impact on glycosylation site occupancy. Nucleotide sugar concentrations may only be critical during extreme starvation. Further work is needed to determine the impact of nucleotide sugars on glycosylation in well-fed cultures.

The authors acknowledge partial financial support from the National Science Foundation (Cooperative Agreement EEC-9402065) and the National Institutes of Health (Grant Number 5T32GM08334).

References

Allen S, Naim HY, Bulleid NJ. 1995. Intracellular folding of tissue-type plasminogen activator: Effects of disulfide bond formation on N-linked glycosylation and secretion. J Biol Chem 270:4797–4804.

Anderson DC, Goochee CF. 1995. The effect of ammonia on the O-linked glycosylation of granulocyte colony-stimulating factor produced by Chinese hamster ovary cells. Biotechnol Bioeng 47:96–105.

Arakawa T, Hsu YR. 1987. Acid unfolding and self-association of recombinant Escherichia coli derived human interferon γ. Biochemistry 26: 5428–5432.

Baumann H, Jahreis GP. 1983. Glucose starvation leads in rat hepatoma cells to partially N-glycosylated glycoproteins including α1-acid glycoproteins. J Biol Chem 258:3942–3949.

Berg DT, Burck PJ, Berg DH, Grinnell BW. 1993. Kringle glycosylation in a modified human tissue plasminogen activator improves functional properties. Blood 81:1312–1322.

Borys MC, Linzer DIH, Papoutsakis ET. 1994. Ammonia affects the glycosylation patterns of recombinant mouse placental lactogen-I by Chinese hamster ovary cells in a pH-dependent manner. Biotechnol Bioeng 43:505–514.

Chapman AE, Calhoun JC. 1988. Effects of glucose starvation and puromycin treatment on lipid-linked oligosaccharide precursors and biosynthetic enzymes in Chinese hamster ovary cells in vivo and in vitro. Arch Biochem Biophys 260:320–333.

Crick DC, Waechter CJ. 1994. Long-chain cis-isoprenyltransferase activity is induced early in the developmental program for protein N-glycosylation in embryonic rat brain cells. J Neurochem 62:247–256.

Cumming DA. 1991. Glycosylation of recombinant protein therapeutics: Control and functional implications. Glycobiology 1:115–130.

Curling EMA, Hayter PM, Baines AJ, Bull AT, Gull K, Strange PG, Jenkins N. 1990. Recombinant human interferon-γ: Differences in glycosylation and proteolytic processing lead to heterogeneity in batch culture. Biochem J 272:333–337.

Datema R, Schwarz RT. 1979. Interference with glycosylation of glycoproteins: Inhibition of formation of lipid-linked oligosaccharides in vivo. Biochem J 184:113–123.

DeFrancesco L, Scheffler IE, Bissell MJ. 1976. A respiration-deficient Chinese hamster cell line with a defect in NADH-coenzyme Q reductase. J Biol Chem 251:4588–4595.

Eigenbrodt E, Fister P, Reinacher M. 1985. New perspectives on carbohydrate metabolism in tumor cells. In: Beitner R, editor. Regulation of carbohydrate metabolism. Boca Raton. FL: CRC Press, Inc.

Elbein AD. 1987. Inhibitors of the biosynthesis and processing of N-linked oligosaccharide chains. Annu Rev Biochem 56:497–534.

Fielder K, Simons K. 1995. The role of N-glycans in the secretory pathway. Cell 81:309–312.

Flesher AR, Marzowski J, Wang W-C, Raff HV. 1995. Fluorophore-labeled carbohydrate analysis of immunoglobulin fusion proteins: Correlation of oligosaccharide content with in vivo clearance profile. Biotechnol Bioeng 46:399–407.

Gawlitzek M, Valley U, Nimtz M, Wagner R, Conradt HS. 1995. Effects of ammonia and glucosamine on the glycosylation pattern of recombinant proteins expressed from BHK-21 cells. In: Beuvery EC, Griffiths JB, Zeijlemaker WP, editors: Animal cell technology: Developments towards the 21st century. Dordrecht, The Netherlands: Kluwer Academic Publishers.

Gershman H, Robbins PW. 1981. Transitory effects of glucose starvation on the synthesis of dolichol-linked oligosaccharides in mammalian cells. J Biol Chem 256:7774–7780.

Goochee CF, Gramer MJ, Anderson DC, Bahr JB. 1992. The oligosaccharides of glycoproteins: Factors affecting their synthesis and their influence on glycoprotein properties. In: Todd P, Sikdar SK, Bier M, editors. Frontiers in bioprocessing II. Washington, DC: American Chemical Society.

Goochee CF, Monica T. 1990. Environmental effects on protein glycosylation. Biotechnology 8:421–427.

Hamilton WG, Ham RG. 1977. Clonal growth of Chinese hamster cell lines in protein-free media. In Vitro 13:537–547.

Hayter PM, Curling EMA, Gould ML, Baines AJ, Jenkins N, Salmon I, Strange PG, Bull AT. 1993. The effect of the dilution rate on CHO cell physiology and recombinant interferon-γ production in glucose-limited chemostat culture. Biotechnol Bioeng 42:1077–1085.

Helenius A. 1994. How N-linked oligosaccharides affect glycoprotein folding in the endoplasmic reticulum. Mol Biol Cell 5:253–265.

Hirschberg CB, Snider MD. 1987. Topography of glycosylation in the

rough endoplasmic reticulum and Golgi apparatus. Annu Rev Biochem 56:63–87.

Holst B, Bruun AW, Kielland-Brandt MC, Winther JR. 1996. Competition between folding and glycosylation in the endoplasmic reticulum. EMBO J 15:3538–3546.

James DC, Freedman RB, Hoare M, Jenkins N. 1994. High-resolution separation of recombinant human interferon-γ glycoforms by micellar electrokinetic capillary chromatography. Anal Biochem 222:315–322.

Jenkins N, Curling EMA. 1994. Glycosylation of recombinant proteins: Problems and prospects. Enzyme Microb Technol 16:354–364.

Kaminskas E. 1979. Ribonucleotide depletion in glucose-deprived tumor cells: The role of RNA synthesis. Biochem Biophys Res Commun 88:1391–1397.

Koch HU, Schwarz RT, Scholtissek C. 1979. Glucosamine itself mediates reversible inhibition of protein glycosylation. Eur J Biochem 94: 515–522.

Kopp K, Noé W, Schlüter M, Werner R, Götz F. 1995. The role of physiological cell parameters and culture conditions on product consistency and glycosylation pattern of recombinant CHO expressed glycoproteins: Interferon omega and tissue plasminogen activator. In: Beuvery EC, Griffiths JB, Zeijlemaker WP. Animal cell technology: Developments towards the 21st century. Dordrecht, The Netherlands: Kluwer Academic Publishers.

Kornfeld R, Kornfeld S. 1985. Assembly of asparagine-linked oligosaccharides. Annu Rev Biochem 54:631–664.

Kornfeld S, Ginsburg V. 1966. The metabolism of glucosamine by tissue culture cells. Experimental Cell Res 41:592–600.

Kozutsumi Y, Segal M, Normington K, Gething M-J, Sambrook J. 1988. The presence of malfolded proteins in the endoplasmic reticulum signals the induction of glucose regulated proteins. Nature 332:462–464.

Lanks KW, Gao J-P, Kasambalides EJ. 1988. Nucleoside restoration of heat resistance and suppression of glucose-regulated protein synthesis by glucose-deprived L929 cells. Cancer Res 48:1442–1445.

Lee AS. 1987. Coordinated regulation of a set of genes by glucose and calcium ionophores in mammalian cells. Trends Biochem Sci 12: 20–23.

Nyberg GB, Balcarcel R, Follstad BD, Stephanopoulos G, Wang DIC. 1998. Metabolism of peptide amino acids by Chinese hamster ovary cells grown in a complex medium. Biotechnol Bioeng 62:324–335.

Pan Y-T, Elbein AD. 1982. The formation of lipid-linked oligosaccharides in Madin–Darby canine kidney cells. J Biol Chem 257:2795–2801.

Pels Rijcken WR, Ferwerda W, Van den Eijnden DH, Overdijk B. 1995. Influence of D-galactosamine on the synthesis of sugar nucleotides and glycoconjugates in rat hepatocytes. Glycobiology 5:495–502.

Rapaport E, Christopher CW, Svihovec SK, Ullrey D, Kalckar HM. 1979. Selective high metabolic lability of uridine, guanosine and cytosine triphosphates in response to glucose deprivation and refeeding of untransformed and polyoma virus-transformed hamster fibroblasts. J Cell Physiol 101:229–236.

Rearick JI, Chapman A, Kornfeld S. 1981. Glucose starvation alters lipid-linked oligosaccharide biosynthesis in Chinese hamster ovary cells. J Biol Chem 256:6255–6261.

Rinderknecht E, O'Conner BH, Rodriques H. 1984. Natural human interferon-γ: Complete amino acid sequence and determination of sites of glycosylation. J Biol Chem 259:6790–6797.

Rosenwald AG, Stoll J, Krag SS. 1990. Regulation of glycosylation: Three enzymes compete for a common pool of dolichyl phosphate in vivo. J Biol Chem 265:14544–14553.

Ryll T, Valley U, Wagner R. 1994. Biochemistry of growth inhibition by ammonium ions in mammalian cells. Biotechnol Bioeng 44:184–193.

Ryll T, Wagner R. 1991. Improved ion-pair high-performance liquid chromatographic method for the quantification of a wide variety of nucleotides and sugar-nucleotides in animal cells. J Chromatogr 570:77–88.

Sareneva T, Pirhonen J, Cantell K, Julkunen I. 1995. N-Glycosylation of human interferon-γ. Glycans at Asn-25 are critical for protease resistance. Biochem J 308:9–14.

Sareneva T, Pirhonen J, Cantell K, Kalkkinen N, Julkunen I. 1994. Role of N-glycosylation in the synthesis, dimerization and secretion of human interferon-γ. Biochem J 303:831–840.

Scahill SJ, Devos R, Van der Heyden J, Fiers W. 1983. Expression and characterization of the product of a human immune interferon cDNA gene in Chinese hamster ovary cells. Pro Natl Acad Sci USA 80: 4654–4658.

Shelikoff M, Sinskey AJ, Stephanopoulos G. 1996. A modeling framework for the study of protein glycosylation. Biotechnol Bioeng 50:73–90.

Stark NJ, Heath EC. 1979. Glucose-dependent glycosylation of secretory glycoprotein in mouse myeloma cells. Arch Biochem Biophys 192: 599–609.

Stryer L. 1988. Biochemistry. 3rd edition. New York: W.H. Freeman and Company.

Thorens B, Vassalli P. 1986. Chloroquine and ammonium chloride prevent terminal glycosylation of immunoglobulins in plasma cells without affecting secretion. Nature 321:618–620.

Traxinger RR, Marshall S. 1991. Coordinated regulation of glutamine: fructose-6-phosphate amidotransferase activity by insulin, glucose, and glutamine. J Biol Chem 266:10148–10154.

Turco SJ. 1980. Modification of oligosaccharide-lipid synthesis and protein glycosylation in glucose-deprived cells. Arch Biochem Biophys 205:330–339.

Ullrey DB, Kalckar HM. 1979. Methods for specific characterization of trace amounts of uridine nucleotides in animal cell cultures. Anal Biochem 95:245–249.

Waldman BC, Oliver C, Krag SS. 1987. A clonal derivative of tunicamycin-resistant Chinese hamster ovary cells with increased *N*-acetylglucosamine-phosphate transferase activity has altered asparagine-linked glycosylation. J Cell Physiol 131:302–317.

Wooden SK, Li L-J, Navarro D, Qadri I, Pereira L, Lee AS. 1991. Transactivation of the *grp78* promoter by malfolded proteins, glycosylation block, and calcium ionophore is mediated through a proximal region containing a CCAAT motif which interacts with CTF/NF-I. Mol Cell Biol 11:5612–5623.

Xie L, Nyberg G, Gu X, Li H, Möllborn F, Wang DIC. 1997. γ-Interferon production and quality in stoichiometric fed-batch cultures of Chinese hamster ovary (CHO) cells under serum-free conditions. Biotechnol Bioeng 56:577–582.

The authors

Gregg B. Nyberg *Process and Product Development, Genetics Institute, One Burtt Road, Andover, Massachusetts 01810 (gnyberg@genetics.com).* Dr. Nyberg is a Staff Engineer II in the Bioreactor Process Development Group at Genetics Institute (a wholly owned subsidiary in the Wyeth–Ayerst Division of the American Home Products Corporation). At the time this paper was written, he was a member of the Biotechnology Process Engineering Center at the Massachusetts Institute of Technology. He received a B.S. degree in chemical engineering and petroleum refining from the Colorado School of Mines in 1992. He subsequently attended MIT, where he was an NIH Biotechnology Training Grant Fellow. After earning his doctorate in 1998, he joined Genetics Institute, where he has worked on process development for the production of recombinant proteins in mammalian cell culture. Dr. Nyberg is a member of the American Institute of Chemical Engineers.

R. Robert Balcarcel *Department of Chemical Engineering, Vanderbilt University, Box 1604, Station B, Nashville, Tennessee 37235 (r.robert.balcarcel@vanderbilt.edu).* Dr. Balcarcel is an Assistant Professor of Chemical Engineering at Vanderbilt University. His current research is in biotechnology—determining the effects of environmental factors on cell physiology, with the aim of improving the production of therapeutic proteins. Dr. Balcarcel received a B.S. degree in chemical engineering in 1993 from the University of California, Berkeley, during which time he received the UC Berkeley Regents Scholarship, became a member of Phi Beta Kappa, and was a NACME/General Electric Scholar. He received a Ph.D. degree in chemical engineering in 1999 from the Massachusetts Institute of Technology (MIT), where he was a National Science Foundation Fellow. This paper was written during his graduate studies at MIT and was the product of a three-way collaboration with Dr. Follstad and Dr. Nyberg (fellow graduate students at the time) and their thesis advisers, Dr. Stephanopoulos and Dr. Wang. Dr. Balcarcel is active professionally and is a member of the American Institute of Chemical Engineers.

Brian D. Follstad *Immunex Corporation, Cell Sciences Department, 51 University Street, Seattle, Washington 98101 (follstad@alum.mit.edu).* Currently, Dr. Follstad is a Senior Process Development Engineer at Immunex in Seattle, Washington. He received a bachelor's degree in chemical engineering from the University of Minnesota in 1994 and a Ph.D. degree in chemical engineering from the Massachusetts Institute of Technology (MIT) in 2000. This paper was written while he was at MIT. His Ph.D. thesis was titled "Metabolic flux analysis and population heterogeneity in mammalian cell culture," and covered the topics of metabolic flux analysis, continuous-culture steady-state multiplicity, population heterogeneity, apoptosis, and mitochondria. Dr. Follstad is an author or coauthor of six technical papers.

Gregory Stephanopoulos *Department of Chemical Engineering, Massachusetts Institute of Technology, 77 Massachusetts Avenue, Cambridge, Massachusetts 02139 (gregstep@mit.edu).* Dr. Stephanopoulos is a Professor of Chemical Engineering at MIT. He received his B.S. degree from the National Technical University of Athens, his M.S. degree from the University of Florida, and his Ph.D. degree from the University of Minnesota, all in chemical engineering. In 1978 he joined the faculty of the California Institute of Technology, where he served as Assistant and Associate Professor until 1985. In 1985 he was appointed Professor of Chemical Engineering at MIT, where he has been since then. During the past twenty years, he has taught courses, written extensively, and carried out research at the interface of engineering and biology. He has investigated fundamentals of metabolic pathways and cellular function while seeking ways for the rational improvement of cellular properties using genetic engineering and methods from molecular biology. He has tried to integrate a rigorous evaluation of the cellular state as a means of assessing the effect of genetic modifications and guiding the design of new ones. This philosophy has been embodied in the definition of the field of metabolic engineering and its industrial and medical applications. Additionally, Professor Stephanopoulos has worked on the cultivation and physiology of mammalian cells in culture, in particular programmed cell death (apoptosis) and glycosylation, as well as control and optimization of fermentation processes. Recently he has initiated a major effort in bioinformatics, defined as the upgrade of the information content of measurements of gene expression, protein content, and metabolic fluxes. Professor Stephanopoulos has authored one book, edited four more, and contributed to more than 180 publications; he holds seven patents. He has been recognized with the Dreyfus Foundation Teacher Scholar Award (1982), the Excellence in Teaching Award (1984), and the AIChE Technical Achievement Award (1984). He has been a

Presidental Young Investigator and the Chairman of the Food Pharmaceutical & Bioengineering Division of AIChE (1992). In 1992 he was elected a Founding Fellow of the American Institute for Medical and Biological Engineering. In 1996 he chaired the first Conference on Metabolic Engineering and gave the inaugural Bayer Lecture on Biochemical Engineering at the University of California at Berkeley. In 1997, he was honored with the FPBE Division Award of the AIChE.

Daniel I. C. Wang *Department of Chemical Engineering, Massachusetts Institute of Technology, 77 Massachusetts Avenue, Cambridge, Massachusetts 02139 (dicwang@mit.edu).* Dr. Wang is an Institute Professor of Chemical Engineering at MIT and the Director of the MIT Biotechnology Process Engineering Center. He received a B.S. in chemical engineering and an M.S. in biochemical engineering, both from MIT, in 1959 and 1961, respectively; and a Ph.D. in chemical engineering from the University of Pennsylvania in 1963. He was a Process Engineer at the U.S. Army Biological Laboratory from 1963 to 1965, joining the MIT faculty in 1965. Professor Wang has received numerous honors and awards. The former include election to the American Academy of Arts and Sciences in 1985 and the National Academy of Engineering in 1986; the latter include Outstanding Teacher Awards from the MIT Graduate School Council in 1972, 1976, and 1989; the William H. Walker Award in 1994 from the American Institute of Chemical Engineers; the Asia-Pacific Distinguished Biochemical Engineer Award in 1994; and the Amgen Biochemical Engineering Award in 1995. Professor Wang has published and lectured extensively (five books and 210 papers), and has served on numerous editorial boards of technical journals, technical committees, advisory panels, and boards. His current research interests are in the production of recombinant proteins and in bioprocess monitoring and control.

Publication of this paper

This paper was originally published on pages 336-347 of *Biotechnology and Bioengineering,* Volume 62, Number 3 (1999) The paper was produced by scanning the original version and contains added biographical sketches of its authors. We gratefully acknowledge permission to include it in this issue.